CSIRO PUBLISHING

International Journal of Wildland Fire **2010**, *19*, 710–724 www.publish.csiro.au/journals/ijwf

Burn severity mapping using simulation modelling and satellite imagery[A]

Eva C. Karau[A,B] *and Robert E. Keane*[A]

[A]USDA Forest Service, Rocky Mountain Research Station, Fire Sciences Laboratory, 5775 Highway 10 West, Missoula, MT 59808, USA.
[B]Corresponding author. Email: ekarau@fs.fed.us

Abstract. Although burn severity maps derived from satellite imagery provide a landscape view of fire impacts, fire effects simulation models can provide spatial fire severity estimates and add a biotic context in which to interpret severity. In this project, we evaluated two methods of mapping burn severity in the context of rapid post-fire assessment for four wildfires in western Montana using 64 plots as field reference: (1) an image-based burn severity mapping approach using the Differenced Normalised Burn Ratio, and (2) a fire effects simulation approach using the FIREHARM model. The image-based approach was moderately correlated with percentage tree mortality but had no relationship with percentage fuel consumption, whereas the simulation approach was moderately correlated with percentage fuel consumption and weakly correlated with percentage tree mortality. Burn severity maps produced by the two approaches had mixed results among the four sampled wildfires. Both approaches had the same overall map agreement when compared with a sampled composite burn index but the approaches generated different severity maps. Though there are limitations to both approaches and more research is needed to refine methodologies, these techniques have the potential to be used synergistically to improve burn severity mapping capabilities of land managers, enabling them to quickly and effectively meet rehabilitation objectives.

Additional keywords: differenced normalised burn ratio, fire effects.

Introduction

Land management agencies in the United States work in accordance with the National Fire Plan and agency guidelines to assess the effects of wildland fire and mitigate damage through rehabilitation activities such as reforestation, erosion control, invasive weed treatment, and habitat restoration (NWCG 2003). This requires accurate, efficient and economical methods to assess the severity of a fire at a landscape scale (Brennan and Hardwick 1999). Burn severity mapping technology is a critical tool in the process of identifying severely burned areas and facilitating prudent implementation of costly rehabilitation and restoration efforts (Lachowski *et al*. 1997; Miller and Yool 2002; Eidenshink *et al*. 2007).

Scientists and managers use burn severity maps for a variety of applications. Spatial maps of fire effects are valuable for delineating fire regimes (Morgan *et al*. 2001), linking landscape patterns and scales of disturbance processes (Turner *et al*. 1994; Chuvieco 1999; Hudak *et al*. 2007*a*), assessing potential for post-fire vegetation recovery or reestablishment (Turner *et al*. 1999; Díaz-Delgado *et al*. 2003; Lentile *et al*. 2007), evaluating wildlife habitat disturbance (Zarriello *et al*. 1995), and gauging the effects of fire on species of concern (Kotliar *et al*. 2003). Burn severity maps can also be used to evaluate if a fire had beneficial consequences to the burned landscape (i.e. an unplanned ecosystem restoration treatment) by comparing historical burn severity distributions with severities contained in the recently burned area (Pratt *et al*. 2006).

In general, there are two major approaches for creating useful burn severity maps: remotely sensed imagery and simulation modelling. Remotely sensed imagery from space and airborne platforms has been used to map burn severity at landscape and regional scales for over two decades (Zarriello *et al*. 1995; Eidenshink *et al*. 2007; Lentile *et al*. 2007) and this technology is clearly useful for spatial post-fire resource management (Greer 1994; Brennan and Hardwick 1999; Sunar and Ozkan 2001). Simulation modelling is another, somewhat newer tool that can provide spatial estimates of fire effects provided high-quality input spatial data layers are available. FIREHARM, a landscape-scale fire effects research model, was designed to produce physically based estimates of fire effects that can then be used to describe burn severity quantitatively (Keane *et al*. 2010). Both approaches have limitations associated with implementation, data availability, required expertise, and potential accuracy (Keane *et al*. 2010). This study compared and contrasted

[A]The use of trade or firm names in this paper is for reader information and does not imply endorsement by the US Department of Agriculture of any product or service. This paper was partly written and prepared by US Government employees on official time, and therefore is in the public domain and not subject to copyright in the USA.

10.1071/WF09018 1049-8001/10/060710

model-based spatial fire effects and satellite-derived burn severity maps using field-measured fire effects as reference.

Background

There is often confusion among scientists and managers involving the terminology used to describe the impacts or effects of fire across a wide variety of ecosystem components (Lentile *et al*. 2006). In the present paper, we use the term *fire severity* similarly to Simard (1991): to denote the magnitude of fire-caused damage to vegetation. Discrete, ordinal indices of fire severity are often used to summarise the complex and interacting effects of a fire (Ryan and Noste 1985). The advantage of these indices is that they integrate a variety of information and summarise it into succinct, intuitive categories. The disadvantage is that they are overly simplistic and rarely address all possible management concerns that require an estimate of severity. For example, a fire severity estimate that emphasises soil erosion potential would use a different classification compared with a severity estimate of fire-caused tree mortality or the amount of surface fuel consumed. These are the biophysically dimensioned measures of the effects of fire that vary on a continuous scale. As this project was primarily focussed on the immediate effects of fire, we use the term *burn severity* somewhat interchangeably with the descriptive term fire severity, but more specifically to describe the magnitude of combined fire effects using an ordinal index value, whether it is derived from a satellite image, a fire effects model, or field-sampled data.

Remotely sensed imagery and fire effects models provide extensive views of fire severity for large regions. Both technologies facilitate generation of quick and inexpensive maps, minimising the need for resource-intensive and potentially dangerous field sampling. Burn severity mapping from remotely sensed imagery involves evaluating spectral reflectance characteristics of landscape features and relating that information to the severity of a fire. For this study, we selected the commonly used Differenced Normalised Burn Ratio (ΔNBR) (detailed in Key and Benson 2006*a*) as our image-based methodology because our primary focus was to assess the comparative utility of simulation modelling and a single satellite-derived burn severity mapping approach.

Computer models for predicting fire effects, such as FOFEM and CONSUME, have been available to fire management for over a decade (Ottmar *et al*. 1993; Keane *et al*. 1994). These models simulate the direct effects of a fire on the vegetation, fuels, and soils for a point in space and produce outputs of these effects as biophysically based variables such as fuel consumption and tree mortality. Keane *et al*. (2010) have implemented FOFEM into a spatial computer model called FIREHARM to develop spatially explicit maps of fire hazard and risk. FIREHARM can also simulate burn severity maps using the same methods used to predict fire hazard.

FIREHARM simulates common measures of fire behaviour, fire danger and fire effects to use as variables to rate fire hazard, and then describes the distribution of these measures over multiple scales of time and space to estimate measures of fire risk by simulating weather and fuel moistures (Keane *et al*. 2010). The fire effects predictions from FIREHARM can also provide important variables to describe burn severity physically. Simulated tree mortality, fuel consumption and soil heating estimates using wildfire fuel and weather conditions will allow the manager to fine-tune management actions to specifically focus burned area rehabilitation efforts based on the type and extent of damage that has occurred.

Although the two technologies share some benefits and capabilities, these approaches differ greatly in process and product (Table 1). The FIREHARM modelling approach provides fire effects measurements in physical units, which are perhaps more meaningful, depending on the project objective, than the unitless index of severity that satellite images provide. The remote sensing-based approach is empirical and physically based on the reflectance characteristics of different features in the image. Both model and image data can be categorised into intuitive burn severity categories, if users need an integrated assessment. Both approaches can be used for rapid assessment situations, yet only FIREHARM has utility as a prognostic tool. Whereas FIREHARM input data are consistent and accessible to users (most spatial layers have already been developed and archived for the nation by the LANDFIRE project (www.landfire.gov, accessed 7 July 2010)), burn severity mapping using remote sensing is dictated by the availability of smoke and cloud-free imagery. Fire effects simulation approaches can generate burn severity maps in a shorter time (i.e. overnight) than remote sensing (i.e. sometimes weeks). Both methods require considerable analyst proficiency and significant computing resources to generate high-quality burn severity maps.

In this project, our objective was to compare and contrast model-based spatial fire effects and satellite-derived burn severity maps using field-measured assessments of fire severity, fuel consumption, and tree mortality as reference. We investigated the possibility of combining these technologies to provide an optimal burn mapping system that integrates a biophysically focussed fire modelling approach and a satellite image-based view of burn severity. Prefire imagery and input data layers serve as the prefire data, while post-fire imagery and model output provide the means for fire effects evaluation.

Methods

This study compared burn severity image-based mapping and modelling approaches by implementing both for a set of wildfires that occurred in western Montana from 2003 to 2005. We list the following procedures as a general overview of the methods used in this effort:

- *Sampled burned areas.* Field data were used to (1) quantify input variables for FIREHARM; (2) provide reference data for satellite imagery severity mapping; and (3) assess the accuracy of both simulation and imagery methods.
- *Gathered satellite-derived burn severity maps.* Imagery was processed by Burned Area Emergency Response (BAER), a US Forest Service and Department of Interior program initiated to provide ΔNBR-based burn severity maps as rapid response tools for post-fire rehabilitation efforts (USFS 1995; Lachowski *et al*. 1997; http://www.nps.gov/fire/fire/fir_baer.cfm).
- *Simulated and mapped burn severity and fire effects.* We used FIREHARM for two different scenarios: (1) 'Plot-based' (parameterisation using individual plots) and (2) 'LANDFIRE-based' (parameterisation using LANDFIRE data).

Table 1. Qualitative comparison of model-based and image-based burn mapping methods

	Fire effects modelling (FIREHARM)	Remotely sensed imagery (ΔNBR)
Fire effects estimation	Provides biophysically based fire effects estimates	An index typically stratified by subjective thresholds into severity classes. Does not directly provide information about biophysical processes or first-order fire effects.
Burn severity maps	Fire effects variables can be mapped as continuous or classed and a thematic burn severity variable is available as output.	Imagery can be displayed as the continuous range of the index or classed into severity categories.
Rapid assessment	Can be quickly run for any time or location, given analyst and input data are current and available.	Imagery may or may not be available immediately post-fire to facilitate rapid assessment and timely burn area rehabilitation.
Predictive capabilities	Could be used as a predictive tool, and can also have fire hazard and risk-mapping capabilities.	Use is limited to post-fire and dependent on suitability of imagery, but derivatives could provide input to spatial models such as for hydrological or erosional processes.
Data archive	Model data can be generated in any volume at any time, given analyst and input data availability.	Archived burn severity data will be readily available from the Monitoring Trends in Burn Severity Project (Extended Assessment only).
System availability	Most simulation models are in the public domain, so users incur no software cost. Most spatial input data will be free and available from LANDFIRE.	Owing to instrument malfunction, satellite overpass frequency, smoke and clouds, or low sun angle, imagery may be unavailable or when needed.
Data preparation	Prefire weather and fuel moisture information must be collected or calculated, and various topographic and ecophysiological data layers must be developed in order to run the model. Severity maps can be prepared rapidly for operational, real-time use.	Many steps are involved in ΔNBR derivation, from acquisition to image calibration, calculation and final classification. Extensive field data may be needed to link to fire severity. Preprocessed data may be freely available, for example from Remote Sensing Applications Center or Monitoring Trends in Burn Severity.
Data quality	FIREHARM output quality depends on input data currency and accuracy as well as model algorithm reliability.	Quality depends on availability, clarity and solar illumination of scenes. Poor results occur with improperly matched pre- and post-fire scenes. Information content depends on whether fire is out, and time since fire of post-fire acquisition.
User resource requirements	Significant computing resources (memory and processor speed) are necessary to run FIREHARM for large landscapes. Geographic Information System software is required for input preparation and map display. Analyst must be familiar with fire effects simulation modelling and GIS.	Significant computing resources (memory and processor speed) are needed to store and manage satellite imagery. GIS and image analysis software is required for data preparation and map display. Image analyst must be familiar with satellite and GIS data management. Users must understand sources of variation within ΔNBR, in addition to fire effects, and recognise problems that can be improved on by proper data selection and processing.

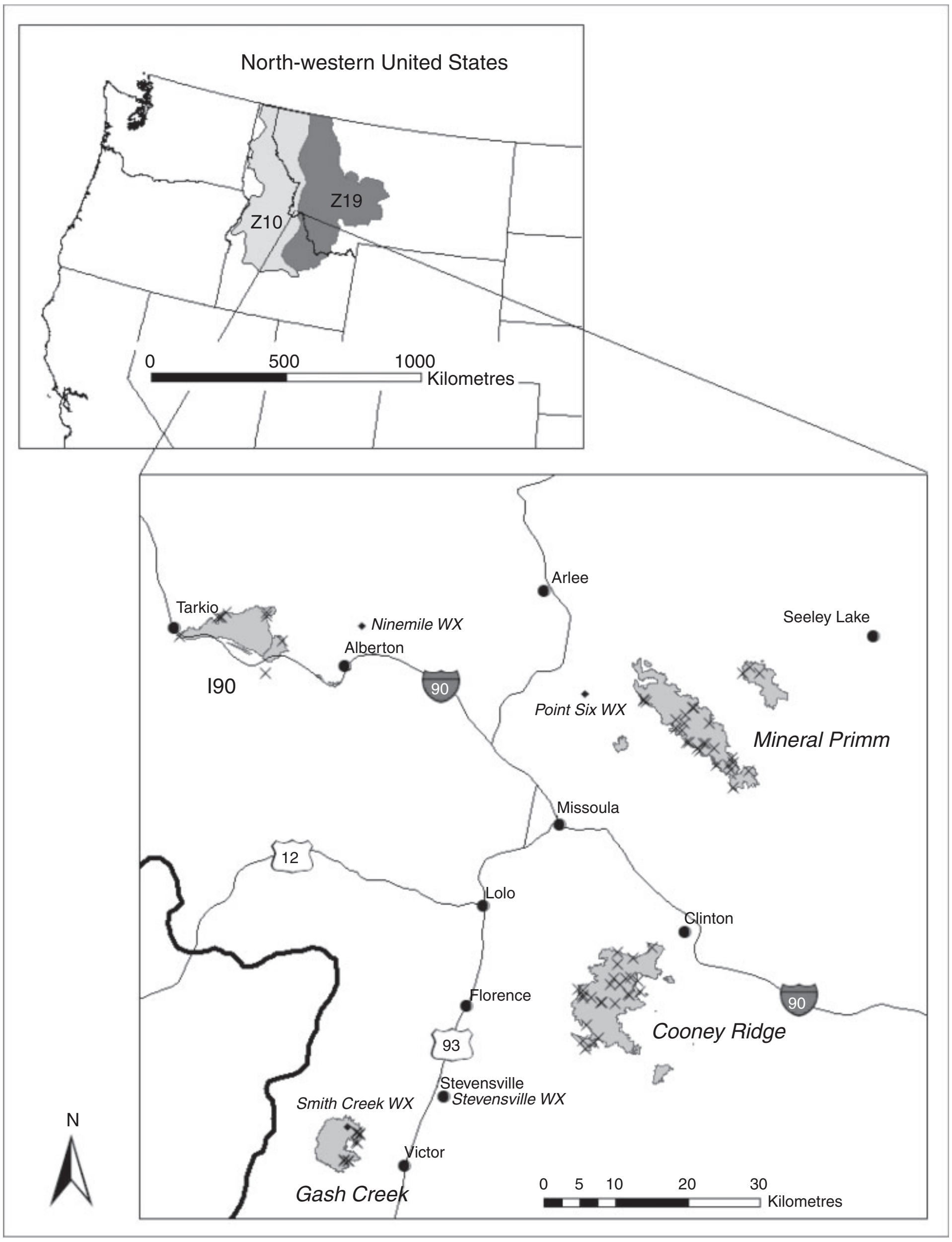

Fig. 1. Map of study areas showing LANDFIRE zones (light grey and dark grey), wildfires (light grey), weather stations (small points) and plot locations (crosses).

- *Validated burn severity for both imagery and modelling methods.*
- *Compared both methods using map agreement and lessons learned from the mapping process.*

Study areas

We selected wildfire areas within LANDFIRE mapping zones 10 and 19. We first sampled the Zone 19 Cooney Ridge and Mineral Primm wildfires, and once LANDFIRE completed Zone 10, we sampled the 2005 I90 Complex and the 2006 Gash Creek fires (Fig. 1). Though the four fires are located in two LANDFIRE zones, they are geographically close (all are within ~60 km of Missoula, Montana, USA). Climate in these Northern Rocky Mountain landscapes is cool temperate, with a minor maritime influence. Mean annual temperature ranges from 2 to 8°C. Summers are dry and precipitation ranges from 410 to over 2540 mm, with most falling as snow in spring, autumn and winter (McNab and Avers 1994). The fires burned through varying topography (valleys, rolling foothills, steep-sided ridges and peaks) ranging from 876 to 2524 m in elevation.

The Mineral Primm and Cooney Ridge fires started in early August of 2003 and each grew to over 10 000 ha by the time they were contained in mid-September (Table 2). Vegetation cover in both fire areas is dominated by temperate coniferous forests and woodlands of Douglas-fir (*Pseudotsuga menziesii*), Engelmann spruce–subalpine fir (*Picea engelmannii–Abies lasiocarpa*) and lodgepole pine (*Pinus contorta*). The I90 fire complex (directly adjacent to Interstate 90) started on 4 August 2005 and burned primarily through Douglas-fir-dominated mixed conifer forests, grassland–herbaceous communities and ponderosa pine forests. The final fire area at containment was reported as 4452 ha. The high-elevation Gash Creek fire was ignited by lightning on 24 July 2006 in the northern Bitterroot Mountains. The fire grew to 3561 ha, burning through landscapes dominated by mid- to high-elevation forest types: Engelmann spruce–subalpine fir, Douglas-fir, whitebark pine and lodgepole pine forests.

Field sampling

We conducted our field sampling within 3 months following the fire dates for the I90 and Gash Creek fires. Owing to scheduling constraints, we had to perform our sampling in the spring and summer following the fire (10–12 months after fire) for the Cooney Ridge and Mineral Primm fires.

As we could only sample fire effects after the wildfires had occurred, it was impossible to obtain a prefire fuel load for our fuel consumption calculations. Instead, we used a paired-plot approach where unburned plots were paired with adjacent burned plots that were similar in site characteristics and vegetation conditions. We centred plots in large (60 × 60-m) areas of homogeneous burn severity, cover type, structural stage, fuel type, slope, aspect, and elevation, well away from roads, trails or other major features. Both natural features (topography, soil type, microclimate, the inherent complexity of burn patterns) and anthropogenic features (fire lines, roads, management units) combined to confound the search for potential plot sites within a homogenous fuel type that included both burned and unburned areas. It was necessary to collect field data from several fire areas as these very specific plot selection requirements made it impossible to establish enough plots in a single fire area.

We used a 404.68-m^2 (0.10-acre) circular plot to define the sampling unit where we recorded plot description information, tallied trees and fuels for all burned and unburned plots, and assessed Composite Burn Index (CBI) only on burned plots. We followed FIREMON protocol (Lutes *et al*. 2006) for all field sampling. For trees, we recorded species, status (healthy, unhealthy or dead), diameter at breast height (DBH) (cm), tree height (m), crown class (open grown, emergent, dominant, codominant, intermediate or suppressed), char height (m) and crown scorch (%), and noted snags (trees dead before the fire) for all dead mature trees (>11.43 cm DBH) in the plot. All trees less than 11.43 cm DBH were counted as saplings and measured at the plot level, where we counted the number of trees in classes defined by species, DBH (cm) and average height (m). For seedlings (trees <1.43 cm DBH, <1.37 m tall), we counted the number of trees in classes (defined in the same way as for saplings) in a 40.47-m^2 (0.01-acre) microplot nested within the macroplot.

For fuel-load sampling, we established as many sampling transects as needed to obtain 100 pieces of down woody debris; at minimum, we established three planes, oriented 90°, 300° and 270° true north. The sampling plane for 1-h and 10-h fuels extended 1.83 m from the 3.05-m mark of the tape, which had

Table 2. Important information for the wildfires used in this study

Fire	Cooney Ridge	Mineral Primm	I90 Complex	Gash Creek
Approximate start date[A]	8 August 2003	6 August 2003	4 August 2005	24 July 2006
Approximate containment date[A]	15 September 2003	19 September 2003	21 August 2005	16 September 2006
Approximate location	18 km E of Florence	31 km NE of Missoula	North of I90, near Alberton	10 km SW of Victor
Size at containment (ha)[A]	10 392	10 199	4452	3561
Cause[A]	Lightning	Unknown	Unknown	Lightning
Weather station: name, location	Stevensville, 46°30′43″N–114°05′33″W	Point Six, 47°02′28″N–113°58′45″W	Ninemile, 47°04′15″N–114°24′08″W	Smith Creek, 46°27′02″N–114°15′10″W
Prefire Burned Area Reflectance Classification image: sensor, date	TM, 10 July 2002	TM, 10 July 2002	TM, 10 July 2002	TM, 11 August 2005
Post-fire BARC image: sensor, date	TM, 31 August 2003	TM, 31 August 2003	ETM+, 19 August 2005	SPOT 4, 1 September 2006
Number of field plot pairs	23	28	8	5

[A]From National Incident Management Coordination Center incident management situation reports.

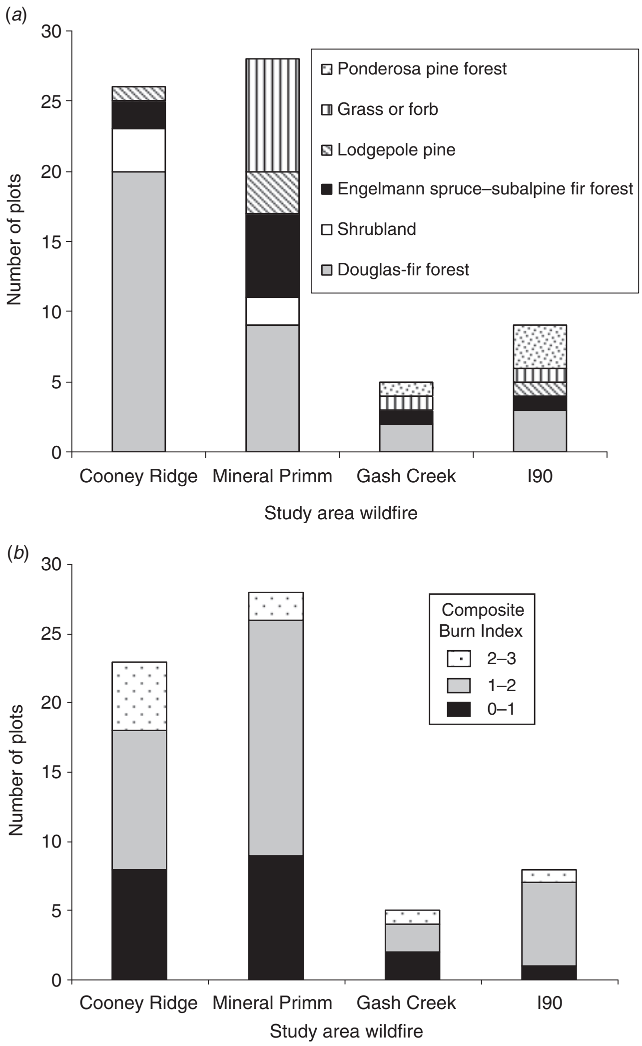

Fig. 2. Distribution of the 64 plots collected in the four wildfire areas across (*a*) vegetation types and (*b*) Composite Burn Index (CBI) scores.

its origin at plot centre. The sampling plane for 100-h fuels extended 3.05 m from the 3.05-m mark of the tape. We counted pieces of each fuel component that crossed the transect and tallied these numbers in the plot sheets. For 1000-h fuels, we tallied the diameter and rot condition (on a five-level scale from sound to rotten, as detailed in Lutes *et al.* 2006) of every log over 7.62 cm in diameter for the entire length of the 18.29-m transect. We estimated vegetation cover and height and took duff and litter depth measurements at the middle (9.14-m mark) and the end (18.29-m mark) of the transect.

Composite Burn Index (CBI), a ground-based burn severity measure designed to relate to the ΔNBR (Key and Benson 2006*b*), was assessed for all burned plots within the plot boundaries. Realising that it is more difficult to assess new seed germination and resprouting when collecting CBI data directly after the fire (with initial assessment timing), we assessed mortality of trees and shrubs based on condition of stems and root crowns to determine whether individual plants were expected to die within 1 or 2 years (Key and Benson 2006*b*). For the Cooney Ridge and Mineral Primm fires, which we sampled 10+ months after fire, we did our best to mentally recreate the immediate post-fire conditions as we did our sampling, in order to follow the initial assessment timing.

Fuel loading, tree mortality and CBI values were calculated in FIREMON and summarised for each macroplot. To calculate fuel consumption (kg m^{-2}) for the field data, we subtracted fuel loads measured on burned plots from those measured on adjacent, paired unburned macroplots. Tree mortality was calculated as the percentage of fire-killed dead trees (greater than 2.5 cm in diameter) on a macroplot. We used measures of fuel consumption and tree mortality as reference data in comparisons with model-derived and image-derived data.

We sampled 23 unburned–burned plot pairs at Cooney Ridge, 28 at Mineral Primm, 8 at I90 and 5 at Gash Creek wildfire areas. The majority of the 64 plots pairs were located in forested vegetation types (49% Douglas-fir, 15% Engelmann spruce–subalpine fir, 7.5% lodgepole pine and 6% ponderosa pine) with fewer plots in grass (15%) and shrub (7.5%) cover types (Fig. 2*a*). Though grass and shrub landscapes together comprised only ~22% of all of our plots, we included them in our analysis to obtain a broad range of fuel loadings and tree densities. We originally intended to sample an equal number of plots in each of three burn severity classes (high, medium and low, as roughly evaluated in the field); however, the limited extent of suitable area to install unburned–burned pairs ultimately dictated plot selection and resulted in a low number of plots and uneven distribution across severity levels as categorised by plot CBI values (Fig. 2*b*).

Satellite imagery

We chose the ΔNBR as calculated from Landsat imagery in Key and Benson (2006*a*) because it appears to be the most commonly tested (and used) image-based severity mapping technique. The ΔNBR showed strong relationships with the CBI, a field-based integrative assessment of burn severity (Cocke *et al.* 2005; Key and Benson 2006*b*), and it was moderately correlated with a range of other field-measured fire effects variables (Hudak *et al.* 2007*b*). The ΔNBR methodology has been used to map severity in a variety of ecosystems and landscapes across the United States (Duffy *et al.* 2007; Lentile *et al.* 2007) and internationally (Escuin *et al.* 2008; but see Roy *et al.* 2006). Finally, ΔNBR is the landscape assessment methodology included in the FIREMON sampling protocol (Key and Benson 2006*a*), which is also used in the present study.

We obtained BAER products for all four fires from the US Forest Service Remote Sensing Applications Center (RSAC). They performed all of the necessary image preparation steps, such as pre and post-fire scene selection, radiometric and terrain correction and spatial co-registration (http://www.fs.fed.us/eng/rsac/baer/). We used RSAC's Burned Area Reflectance Classification (BARC256) product (http://www.fs.fed.us/eng/rsac/baer/barc.html) for our comparison because it represents ΔNBR as a continuous variable, scaled such that values range from 0 to 255 with increasing burn severity. In BARC256 calculation, the prefire scene is typically chosen from all scenes captured during the year before the post-fire scene, ideally during a phenologically similar period. With one exception listed below, our prefire images were from the year before the fire and post-fire images from directly after the fire, following 'initial assessment' timing (Key and Benson 2006*b*). This image timing is consistent with the BAER 'rapid assessment' and our objective of testing a system for collecting and evaluating data immediately after a fire.

BARC analysts are under pressure to select, process and deliver images quickly to managers, so it is possible that more appropriate options for pre- and post-fire image selections are overlooked and burn perimeters are delineated in haste. Inconsistency exists in BARC products owing to instrument malfunction, timing of satellite overpass, or smoke or cloud obstruction at the time an image is critically needed. Several BARC quality issues affect the imagery used in this project:

- Phenology is somewhat mismatched between the pre- and post-fire images for the Cooney Ridge and Mineral Primm fires.
- The prefire image for the I90 fire is from 3 years before the fire owing to a lack of cloud-free prefire images in this area.
- The Cooney Ridge fire was still burning during acquisition of the post-fire scene, producing smoke in the image.
- The I90 post-fire image is from the Landsat Enhanced Thematic Mapper Plus sensor, which has a malfunction that causes lines of missing data.
- The post-fire image for the Gash Creek fire was acquired from the SPOT 4 (Satellite pour l'Observation de la Terre) satellite, presumably because acceptable Landsat images were unavailable.

We chose to use the BARC products 'as is' with the intention of conducting our comparison analysis using products that managers might realistically expect to obtain on a fire. Neither the BARC nor the FIREHARM maps of fire severity are considered superior or as a reference; both were evaluated as potential burn severity mapping products.

In our validation analysis, we used the continuous ΔNBR data (BARC256) to examine relationships between ΔNBR and field-measured variables, but to assess map agreement, we sliced the BARC256 into three classes to match the three FIREHARM burn severity classes using Jenks natural breaks (McMaster 1997). We chose the Jenks method as it is an efficient, consistent and repeatable way to slice the full range of pixel values into a three-category burn severity index.

FIREHARM simulations

FIREHARM requires several input data layers to compute spatial fire effects variables and burn severity. The most important of these for this study include digital maps of topography (elevation, aspect, slope), vegetation (tree attributes, cover type) and fuels (fuel loading) along with site-specific weather and fuel moisture estimates. These inputs are passed to the FOFEM model embedded in the FIREHARM program to generate estimates of tree mortality, fuel consumption, smoke emissions, and soil heating. Most of the FIREHARM input data are available for the continental United States from the National LANDFIRE Mapping Project (www.landfire.gov). LANDFIRE is a multiagency effort to provide land managers with comprehensive spatial data and planning-focussed analysis tools. In some cases, managers may need to independently create the input data layers required to run FIREHARM but that is cost, time and resource prohibitive (Reinhardt *et al.* 2001). However, the availability of LANDFIRE data layers enables managers to run FIREHARM to generate fire hazard and burn severity maps with relative ease.

Table 3. FIREHARM weather and fuel moisture input values

	Cooney Ridge	Mineral Primm	I90 Complex	Gash Creek
Minimum temperature (°C)	26.6	28.3	30.6	23.4
Maximum temperature (°C)	11.0	7.2	8.8	10.9
Relative humidity (%)	35	29	23	33
Wind speed (km h^{-1})	6	11	10	6
Wind direction (azimuth)	237	180	180	90
1-h fuel moisture (FM) (%)	5	6	4	6
10-h FM (%)	6	10	5	7
100-h FM (%)	12	13	9	8
1000-h FM (%)	12	14	10	13
10 000-h FM (%)	0	0	0	0
Foliar moisture (%)	100	100	100	100
Litter moisture (%)	5	6	4	6
Duff moisture (%)	75	75	75	75
Herbaceous moisture (%)	65	79	41	66
Shrub moisture (%)	88	107	72	97

We simulated two scenarios using the FIREHARM model. The 'plot-based' simulations were used to *validate* FIREHARM and ΔNBR. They represent the most realistic evaluation of model capabilities, given the availability of accurate input information. We conducted 'LANDFIRE-based' simulations to *demonstrate* the landscape mapping capabilities and to replicate how FIREHARM would be used in operational settings without the availability of specific plot data for model parameterisation.

Plot-based simulations

For this scenario, we used the field data from each of the 64 plots in the four fire areas to parameterise and initialise FIREHARM explicitly for the simulation of fire effects. We took the following inputs directly from the plot data forms: slope, aspect, elevation, vegetation type and geographic position (latitude and longitude). Because the Scott and Burgan (2005) Fire Behaviour Fuel Models were not available when we began our field sampling, we overlaid plot locations with LANDFIRE spatial data to obtain the Scott and Burgan (2005) fuel models. We used the sampled tree information to create the tree list input to FIREHARM to calculate tree mortality (Keane *et al.* 2010). The tree list requires the following fields: species, density (number of trees km^{-2}), DBH (cm), tree height (m), canopy base height (m), crown class and tree status (healthy, unhealthy or dead). Because we wished to simulate tree mortality on our burned plots, we modified our collected data for burned plots to change the status of all trees that were killed by the fire from 'dead' to 'healthy'; snags (trees that were dead before the fire) retained a 'dead' status. Because we could not collect canopy base height information on the dead trees, we estimated this value as a function of tree height using FOFEM default values (Reinhardt *et al.* 1997). To parameterise prefire fuel loads, we queried our field data (using FIREMON) to calculate fuel loadings for each plot by sampled fuel components (1-, 10-, 100-, 1000-h, litter and duff loads (kg m^{-2})).

For FIREHARM weather input, we gathered several types of weather and fuel moisture information during the burning period at our fire areas: (1) maximum temperature (°C); (2) minimum temperature (°C); (3) relative humidity (%); (4) wind speed (miles h^{-1}); (5) wind direction (azimuth) and fuel moistures for each fuel component (Table 3). We accessed Kansas City Fire Access software through the National Fire and Aviation Management web access to obtain the necessary temperature, humidity, and wind information from weather stations at or near each of our four fire areas (Fig. 1; Table 2). We then ran Fire Family Plus (Main *et al*. 1990) to estimate fuel moisture conditions for 1-, 10-, 100-, 1000-h, herb and shrub components. We estimated live foliar moisture (set at 100%), litter moisture (set equal to 1-h fuel moistures), and duff moisture (75%), as these values were not measured on our fires, nor are they products of the National Fire Danger Rating System (Burgan 1979). We averaged the weather and fuels values through the record of the fire period (from ignition through containment) to obtain the single value (for each parameter) necessary to populate the weather and fuel moisture input file.

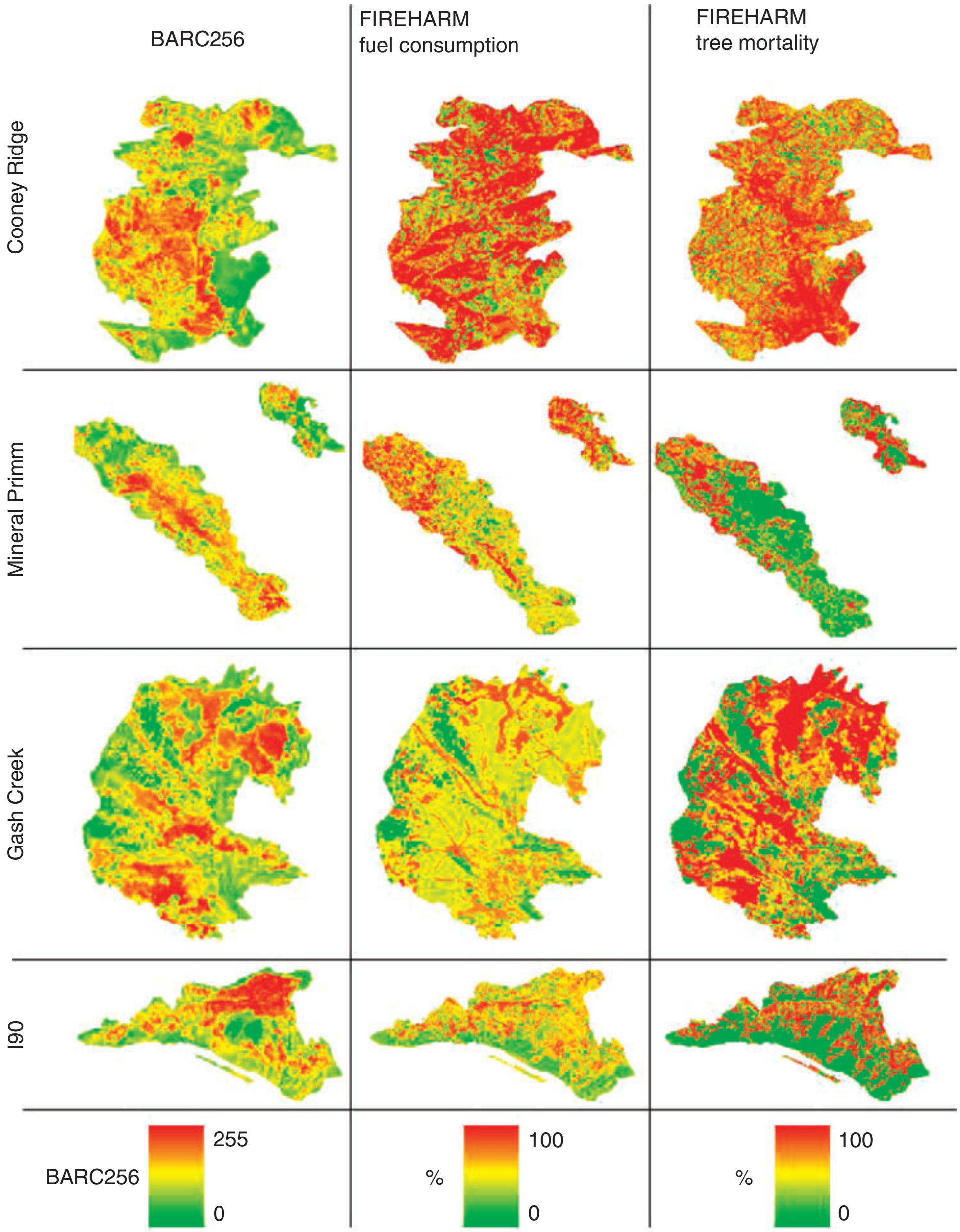

Fig. 3. Maps of burn severity and fire effects for the four fire areas (arranged in rows from first to last: Cooney Ridge, Mineral Primm, Gash Creek and I90 Complex). Column 1: BARC256 (ΔNBR (Differenced Normalised Burn Ratio) scaled from 0 to 255 (unclassed)). Column 2: FIREHARM-simulated fuel consumption (%). Column 3: FIREHARM-simulated TREE Mortality (%).

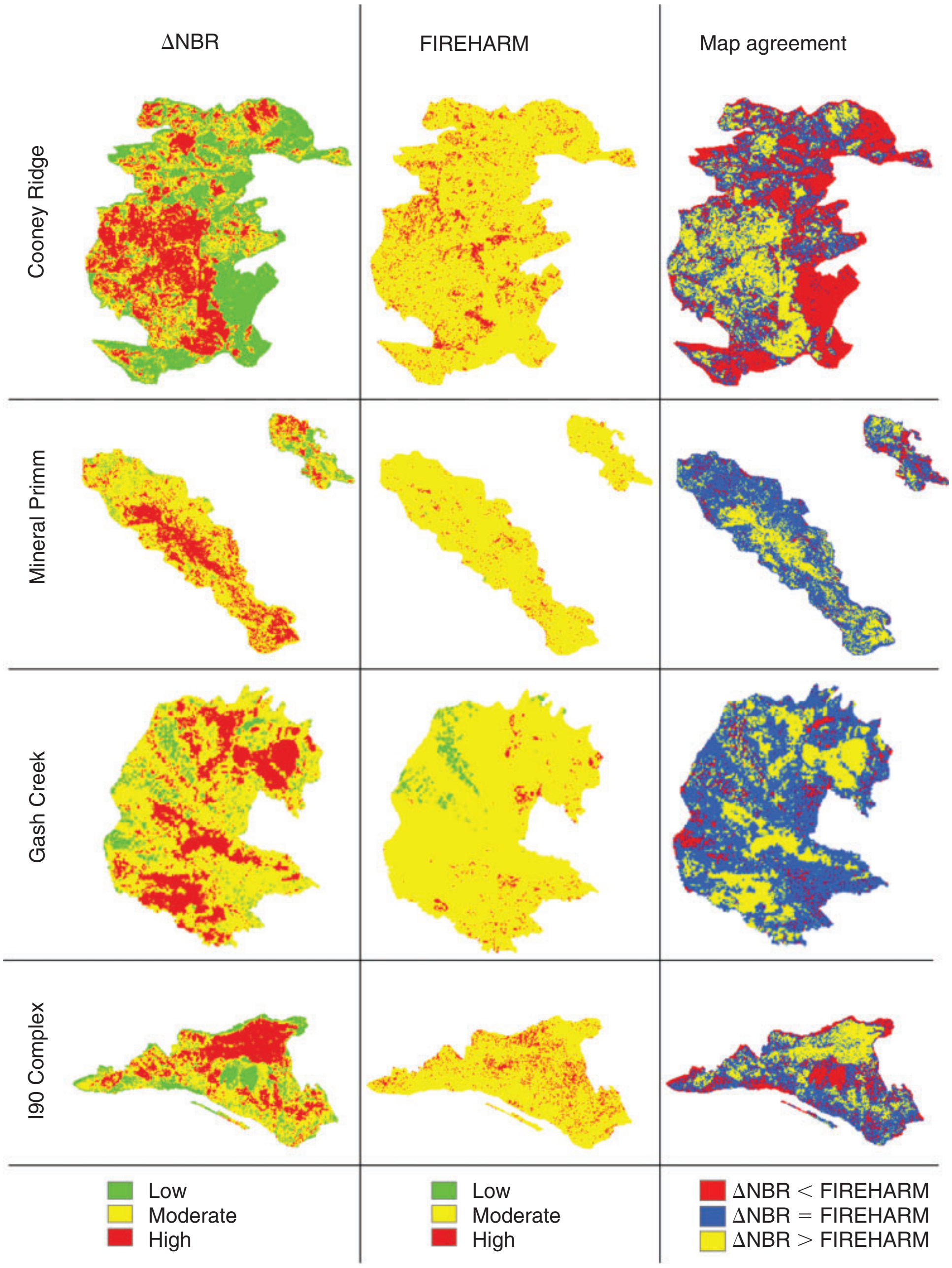

Fig. 4. Satellite-derived and model-simulated maps of burn severity for the four fire areas (arranged in rows from first to last: Cooney Ridge, Mineral Primm, Gash Creek and I90 Complex). Column 1: ΔNBR (Differenced Normalised Burn Ratio) (classed as Low, Moderate and High Burn Severity). Column 2: FIREHARM Burn Severity (classed as Low, Moderate and High Burn Severity). Column 3: difference map showing discrepancy and agreement between ΔNBR and FIREHARM burn severity maps (red means ΔNBR severity was lower than FIREHARM severity, blue means the maps are in agreement, and yellow means ΔNBR severity was higher than FIREHARM severity).

LANDFIRE-based simulations

To demonstrate the rapid mapping capabilities of FIREHARM, the model was parameterised using LANDFIRE spatial data. The following LANDFIRE layers from mapping Zone 19 (for Cooney Ridge and Mineral Primm fires) and Zone 10 (for I90 and Gash Creek fires) were used as input: Existing Vegetation Type, Fire Behaviour Fuel Model, Fuel Loading Model, elevation, slope and aspect (www.landfire.gov). Tree information came from the LANDFIRE tree list spatial data layer that summarises tree information from all plots in the LANDFIRE reference database (Drury and Herynk, in press). We generated all other FIREHARM inputs (weather and fuel moisture) as described for the above plot validation parameterisation.

Table 4. Overall agreement between Differenced Normalised Burn Ratio (ΔNBR)-classified data and FIREHARM burn severity-classified data for the four wildfire areas
Values are from error matrices

Fire area	Agreement (%)
Cooney Ridge	33.5
Mineral Primm	64.8
Gash Creek	63.9
I90 Complex	48.1

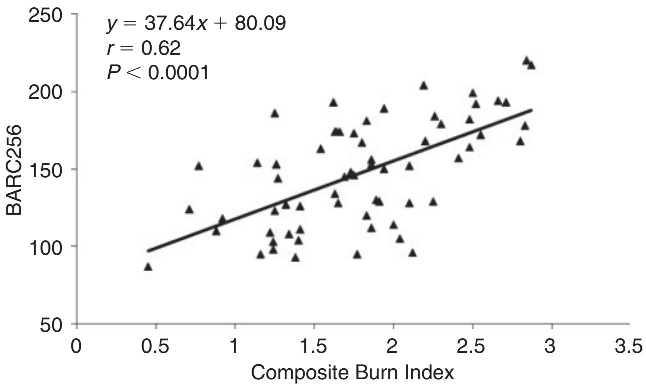

Fig. 5. Relationship between BARC256 (continuous ΔNBR (Differenced Normalised Burn Ratio)) and Composite Burn Index. The solid black line is the linear regression trend line.

We simulated and mapped three FIREHARM fire effects output variables for both parameterisation scenarios in this study:

1. *Fuel consumption.* We calculated the amount of fuel consumed as follows:

$$\text{Fuel consumption} = \frac{FC_{Pred} \times FL_{Pre\text{-}burn}}{100}$$

where FC_{Pred}, FIREHARM-predicted fuel consumption (%), a continuous variable reported by the model as the percentage of the prefire fuel load that is consumed. $FL_{Pre\text{-}burn}$, prefire fuel load (kg m^{-2}). For the individual plot parameterisation scenario, these values are taken directly from the plot data; for the LANDFIRE parameterisation, the values are from the LANDFIRE fuel loading model.
2. *Tree mortality*. A continuous variable reported as the percentage of the total number of trees (saplings and mature trees) on a plot that died owing to fire.
3. *Burn severity*. A categorical variable that integrates several fire effects. Keane *et al*. (2010) compute fire severity based on classes of tree mortality (<40, 40–70, >70%), fuel consumption (<20, 20–50, >50%), and soil heating (<60°C at 2 cm, 60–250°C at 2 cm, >250°C at 2 cm).

Results

Maps of BARC256, simulated fuel consumption, and simulated tree mortality exhibit markedly different spatial patterns across the landscape (Fig. 3). For this analysis, simulated variables are continuous and unclassed; BARC256 is continuous and scaled from 0 to 255.

When comparing categorised burn severity maps, it is clear that ΔNBR- and FIREHARM-modelled burn severity maps vary in agreement across all four fires (Fig. 4). Here, BARC256 was classed using Jenks natural breaks and CBI was rounded to 1, 2 and 3 to represent three burn severity classes: low, moderate and high. Map agreement values range from 33.5% for the Cooney Ridge fire to 64.8% for Mineral Primm (Table 4). We found a moderate relationship between continuous (unclassed) BARC256 and unclassed CBI ($r = 0.62$, $P < 0.0001$) (Fig. 5).

We found a wide range in the strength of relationships between observed fuel consumption and FIREHARM-simulated fuel consumption. Associations were much stronger when the model was parameterised from our plot data ($r = 0.92$) than with the LANDFIRE-based scenario ($r = 0.24$) (Fig. 6*a*). We found a weak relationship between observed fuel consumption and BARC256 ($r = 0.17$) (Fig. 6*b*) and there are three data outliers that further weaken this relationship. These points represent plots that we suspect had a relatively poor burned–unburned fuel consumption match, as the unburned 1000-h fuel loads are much greater than those for the burned plots.

The LANDFIRE-based FIREHARM simulations of percentage tree mortality had a stronger relationship with observed tree mortality ($r = 0.37$) than did the plot-based parameterisation ($r = 0.18$) (Fig. 6*c*). Tree mortality had a moderate positive correlation with BARC256 ($r = 0.53$) (Fig. 6*d*). The tree mortality and fuel consumption predictions were used in the computation of simulated burn severity.

We graphically compared BARC256 and FIREHARM-simulated fire effects variables within severity classes to evaluate if data points might cluster into zones of high, moderate and low severity based on CBI classes. We did this across our set of 64 points using the CBI (rounded to the nearest 1, 2, or 3, corresponding to low, moderate and high severity) to stratify the points (Fig. 7). When BARC256 is plotted against FIREHARM tree mortality and fuel consumption, there appears to be enough separability to distinguish at least between the high burn severity class and the two lower classes; the low and the moderate classes are indistinct from one another (Fig. 7). This is true for both of the simulation parameterisation situations (LANDFIRE-based and plot-based).

Accuracy assessment showed that ΔNBR and FIREHARM simulated burn severity maps had the same level of overall agreement (57.8%) (Table 5), but agreement as measured by kappa analysis (Congalton and Green 1999) for the ΔNBR map was poor (kappa = 0.28, $P = 0.003$). We could not calculate kappa statistics for the FIREHARM burn severity map because there were no FIREHARM-simulated plots classified in the low category. Given the number and distribution of our field reference plots, the comparison accuracy assessment only reflects the accuracy of our sample; it does not represent the general accuracy of FIREHARM or BARC products.

Discussion and conclusions

This study demonstrated that image- and model-derived burn mapping methodologies, used individually or in tandem, have the potential to improve our ability to understand the composition

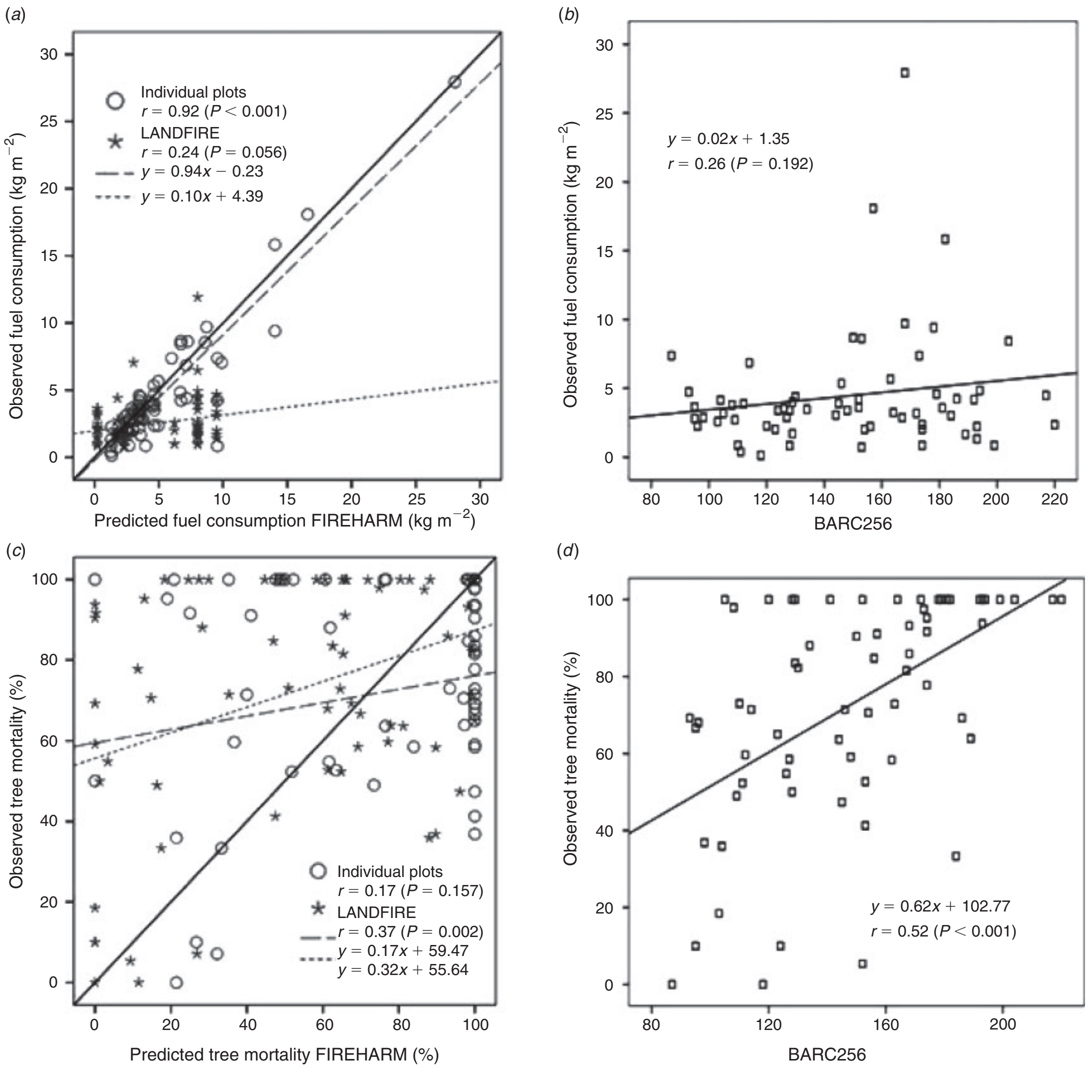

Fig. 6. Relationships between observed and predicted variables for (*a*) observed field-measured *v.* simulated fuel consumption; (*b*) observed fuel consumption *v.* BARC256 (continuous ΔNBR (Differenced Normalised Burn Ratio)); (*c*) observed *v.* simulated tree mortality; and (*d*) observed tree mortality *v.* BARC256. The small-dash and large-dash lines represent the regression trend lines for the FIREHARM simulations using LANDFIRE-parameterised and individually parameterised data respectively. The solid black line is the 1 : 1 line.

of effects resulting from wildfires and perhaps provide a more comprehensive burn severity map product. Burn severity maps created using simulation provide a quick and comprehensive description of fire severity, but results may be suspect because of the low accuracy of the input layers, the complex nature of a spreading fire, and misrepresentation of weather and fuel conditions at the time of burning. However, satellite-derived burn severity maps appear acceptable as spatial indicators of composite fire effects over large areas, but the severity assessment (1) is not based on physical measures of specific fire effects; (2) depends on analyst proficiency and requires that appropriate pre- and post-fire imagery is available for the burned area; and (3) cannot be produced prefire to predict burn severity. Both approaches have distinct advantages and significant limitations (Table 1). It is interesting and potentially useful that where the model performed poorly (predicting tree mortality), the imagery performed relatively well, and where the model performed relatively well (predicting fuel consumption), the imagery performed poorly (Fig. 6).

Agreement between the ΔNBR and FIREHARM burn severity maps is heavily influenced by the large areas of moderate severity in the FIREHARM maps (Fig. 3; Table 5), which may boost the overall map agreement (Table 4). In the case of the Cooney Ridge fire, BARC256 shows a large area of low severity that is classified as moderate severity by FIREHARM (Fig. 3). It may be that the fire severity classification in Keane *et al*. (2010) does not perform well for low-severity fires.

We suspect that BARC data quality issues also impact map agreement results. The BARC pre- and post-fire images used in this study had problems ranging from phenology mismatch to smoke contamination, all of which affect burn severity values. In the case where the post-fire scene is from a completely

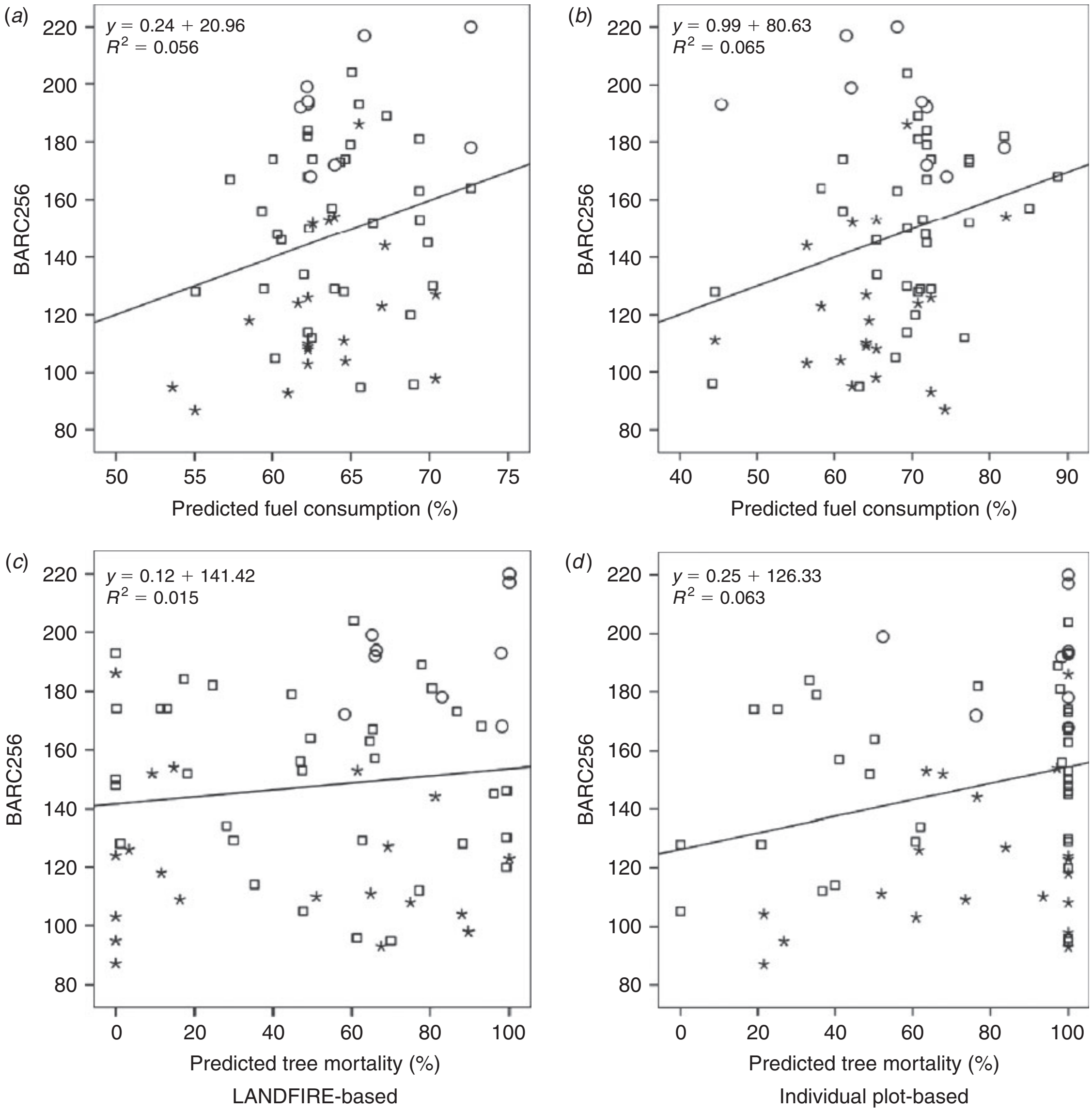

Fig. 7. Relationship between BARC256 (continuous ΔNBR (Differenced Normalised Burn Ratio)) and FIREHARM-modelled fuel consumption (*a*, *b*) and tree mortality (*c*, *d*) for both LANDFIRE (*a*, *c*) and individual plot (*b*, *d*) parameterisations. Circles, squares and stars represent Composite Burn Index (CBI) = 3, 2 and 1 respectively. The solid black lines are the linear regression trend lines.

different satellite, issues of inconsistent radiometric resolution and spatial registration may further confound burn severity representation. For several fires, unburned areas exist within the fire perimeters that were not accounted for in the BARC images. Agreement between BARC and FIREHARM maps may have been different had these areas been excluded from both maps. We caution BARC data end-users to be aware of the potential for poor-quality burn severity map products in a rapid assessment situation. For instance, users may want to ensure that measures were taken to minimise effects of sun angle, phenology mismatch and smoke or cloud contamination in pre and post-fire images (among other issues listed in Table 1).

It is encouraging that under both FIREHARM scenarios, the combination of BARC256 and simulated fire effects variables seems to cluster into somewhat discernable burn severity classes, at least in the high-severity case (Fig. 7). These findings suggest that the two systems might be paired to improve evaluations of fire effects, especially as neither is notably superior in terms of accuracy (Table 5) or utility (Table 1). The model may have utility in cases where satellite imagery is not available and could provide context to image-derived burn severity classifications.

The comparison of CBI with ΔNBR and FIREHARM burn severity is really not a true evaluation of accuracy. CBI is a standardised method that was designed to provide a severity context in which to interpret ΔNBR (Key and Benson 2006*b*). It is based on the combination of visual and structural characteristics that may not be individually detectable as fire

Table 5. Cross-tabulation of Composite Burn Index (CBI) (columns) and classified burn severity maps (rows) for the 64 plots

	Low	Moderate	High	Total
Differenced Normalised Burn Ratio				
Low	2	7	0	9
Moderate	3	20	6	29
High	0	11	15	26
Total	5	38	21	64
Overall sample accuracy (%)				57.8
FIREHARM				
Low	0	0	0	0
Moderate	4	33	17	54
High	1	5	4	10
Total	5	38	21	64
Overall sample accuracy (%)				57.8

effects when viewed by a satellite (Kasischke *et al*. 2008). The fire severity index as computed in FIREHARM, however, is based on simulated tree mortality and fuel consumption. As a result, the three ordinal categories of the CBI, ΔNBR burn severity, and FIREHARM fire severity are not directly comparable so we could not perform a consistent and comprehensive accuracy assessment. However, we included this analysis because CBI ground data are currently the most commonly used map validation method (van Wagtendonk *et al*. 2004; Cocke *et al*. 2005; Epting *et al*. 2005; Key and Benson 2006*b*; Miller and Thode 2007). We feel it provides important information regarding the performance of each map product, if only qualitatively; it shows that overall map accuracy for our sample, assessed with CBI (given the limitations of this method and the constraints of our study), is identical for the ΔNBR and FIREHARM maps (Table 5). We suspect that the low kappa score for this assessment between CBI and ΔNBR may be due to (1) the low total number of field plots that we sampled, and (2) uneven plot distribution through the range of severity.

The strong performance by FIREHARM in predicting fuel consumption is partially due to our ability to parameterise the model's fuel module with actual plot data. Data with this level of detail may be difficult to obtain by the average user who uses LANDFIRE fuel loading model data to parameterise FIREHARM. Our results show that the coarse scale of the LANDFIRE inputs would likely introduce additional error in model predictions, because fuel loadings are more highly variable. Correspondingly, our fuel loading results would likely have been even stronger had we been able to measure actual prefire loadings, instead of using a similar plot as a prefire surrogate. We suspected that using this paired-plot approach would contribute error to our field-based fuel consumption estimates and this would consequently effect the degree of association between ground reference with modelled and satellite burn severity estimates, but there was no alternative fuel sampling methodology. Another source of error is our inability to capture fire spread and fuel dynamics owing to the incompatible sampling scale.

The prediction of FIREHARM-simulated tree mortality and fuel consumption as calculated with field data or LANDFIRE products has several potential limitations:

- *Fire intensity*. FIREHARM predicts fire behaviour assuming a heading fire, which results in increased tree mortality. The dynamics of flanking or backing fires (which occur on natural landscapes) are not captured in the model and this explains why the model often predicts 100% tree mortality.
- *Scorch height*. FIREHARM uses one measure of scorch height for the entire pixel whereas real fires tend to have high variability in scorch height within a small area. This affects the ability of the model to predict whether a crown fire occurs, and if so, what type of fire behaviour will result (running or dependent).
- *Weather information*. In some cases, the weather stations that we used to estimate fuel moisture inputs were distant from the fire (up to 25 km). We suspect that predictions may have been better if weather data were available at a fine spatial scale.
- *Fuels*. Fuel loadings and characteristics vary at finer scales than both the plot measurements and the LANDFIRE mapping products.
- *Paired-plot approach*. Prefire fuel conditions of burned areas may not have been fully represented by sampling an adjacent unburned area.
- *Inaccurate spatial input layers*. In the end, this entire fire severity simulation method ultimately depends on the quality of the input layers. In this study, we used the LANDFIRE input layers because those are the layers that fire management would use if they employed our process in an operational sense. For our study area, these LANDFIRE layers were inaccurate. Our data have indicated that the fuels and vegetation layers range from 20 to 60% accurate. This explains the majority of the inaccuracy in the FIREHARM simulations. The fire behaviour and effects algorithms in FIREHARM have been extensively tested and model predictions are often over 90% correct. Therefore, most of the error in the FIREHARM predictions can be attributed to poor input data and inadequate weather representation.

We believe that the coarseness of the input data and the generality of some of the model algorithms (Keane *et al*. 2010) preclude our modelling efforts from thoroughly capturing fine-scale variability of fire effects to create highly accurate burn severity maps, though we are encouraged by strong correlations between observed and simulated fuel consumption.

Considering satellite–sensor–target relationships, it is not surprising that we found a weak correlation between BARC256 imagery and fuel consumption, and moderately high correlations between BARC256 and CBI and between BARC256 and tree mortality. It makes intuitive sense that a satellite image would do a better job of capturing the dynamics of the overstorey (first layer of material 'seen' by the sensor) than the understorey that is obscured by this top layer. This is consistent with Epting *et al*. (2005), who found imagery was highly correlated with burn severity in only forested cover types, and both Hudak *et al*. (2007*b*) and Hoy *et al*. (2008), who found overstorey measures of canopy condition were more highly correlated with imagery than understorey measures. Similarly, if we were to stratify the analysis by vegetation type, we would expect to see stronger CBI–BARC256 relationships in forested *v.* shrub or grass landscapes. For these reasons, and also because all of the fires in our study were located in the US Northern Rockies, we caution readers against extrapolating these results to ecosystems dominated by shrubs or grass or even to other forested regions owing to differences in forest species and structure.

We feel that both satellite imagery and modelling approaches are of great value to fire management depending on time, place, resources, and available data (Table 1). Real-time assessments of fire effects can be successfully accomplished using a modelling approach whereas long-term severity assessments for rehabilitation efforts could use the image data. Image data can also be combined with the simulated results to provide a physical basis for understanding and interpreting patterns of severity. For example, ΔNBR maps could be overlaid with predicted fuel consumption and tree mortality maps to develop ΔNBR thresholds to delineate burn severity classes in the absence of field data. Moreover, burn severity from imagery could be cross-referenced with predicted fire effects to tailor the burn severity for a specific management application. The ΔNBR maps, for instance, can be cross-referenced with FIREHARM output to determine areas of high tree mortality and deep soil heating. Based on our data, neither approach on its own would likely suit all the multifaceted needs desired by fire and land management, but the integration of both approaches may lead to a synergy in the understanding and assessment of fire severity, especially as more comprehensive data and more accurate fire effects models become available.

Imagery and simulation can be effective to map fire severity if the target conditions are understood and well defined, and reflect the potential detection capabilities of the technology. The main problem with comparing imagery with simulation is that the two methodologies use disparate classifications. Future research efforts should endeavour to create definitions and classifications of fire severity that not only correlate with imagery but also represent the biophysical properties that drive fire effects.

Acknowledgements

This effort was funded by the Joint Fire Sciences Program Agreement 05-1-1-12. We thank Jason Herynk, of Systems for Environmental Management, and Stacy Drury, Violet Holley, Greg Cohn, Curtis Johnson, Jhen Rawling and Signe Leirfallom, Rocky Mountain Research Station, Missoula Fire Sciences Laboratory. We also thank the anonymous reviewers whose comments and suggestions greatly improved the manuscript.

References

Brennan MW, Hardwick PE (1999) Burned Area Emergency Rehabilitation teams utilize GIS and remote sensing. *Earth Observation Magazine* **8**(6), 14–16. Available at http://web.archive.org/web/20071116214324/www.eomonline.com/archives.php [Verified 7 July 2010]

Burgan RE (1979) Estimating live fuel moisture for the 1978 National Fire Danger Rating System. USDA Forest Service, Intermountain Forest and Range Experiment Station, General Technical Report INT-167. (Ogden, UT)

Chuvieco E (1999) Measuring changes in landscape pattern from satellite images: short-term effects of fire on spatial diversity. *International Journal of Remote Sensing* **20**(12), 2331–2346. doi:10.1080/014311699212056

Cocke AE, Fule PZ, Crouse JE (2005) Comparison of burn severity assessments using Differenced Normalized Burn Ratio and ground data. *International Journal of Wildland Fire* **14**, 189–198. doi:10.1071/WF04010

Congalton R, Green K (1999) 'Assessing the Accuracy of Remotely Sensed Data: Principles and Practices.' (CRC/Lewis Press: Boca Raton, FL)

Díaz-Delgado R, Lloret F, Pons X (2003) Influence of fire severity on plant regeneration by means of remote sensing imagery. *International Journal of Remote Sensing* **24**(8), 1751–1763. doi:10.1080/01431160210144732

Drury SA, Herynk J, Nat Tree: a national spatially explicit tree list from LANDFIRE data. USDA Forest Service, Rocky Mountain Research Station, General Technical Report, in press.

Duffy PA, Epting J, Graham JM, Rupp TS, McGuire DA (2007) Analysis of Alaskan burn severity patterns using remotely sensed data. *International Journal of Wildland Fire* **16**(3), 277–284. doi:10.1071/WF06034

Eidenshink J, Schwind B, Brewer K, Zhu Z, Quayle B, Howard S (2007) A project for monitoring trends in burn severity. *Fire Ecology* **3**(1), 3–21. doi:10.4996/FIREECOLOGY.0301003

Epting J, Verbyla D, Sorbel B (2005) Evaluation of remotely sensed indices for assessing burn severity in interior Alaska using Landsat TM and ETM+. *Remote Sensing of Environment* **96**, 328–339. doi:10.1016/J.RSE.2005.03.002

Escuin S, Navarro R, Fernandez P (2008) Fire severity assessment using NBR (Normalized Burn Ratio) derived from LANDSAT TM/ETM images. *International Journal of Remote Sensing* **29**(4), 1053–1073. doi:10.1080/01431160701281072

Greer JD (1994) GIS and remote sensing for wildland fire suppression and burned area restoration. *Photogrammetric Engineering and Remote Sensing* **60**(9), 1059–1064.

Hoy EE, French NHF, Turetsky MR, Trigg SN, Kasischke ES (2008) Evaluating the potential of Landsat TM/ETM+ imagery for assessing fire severity in Alaskan black spruce forests. *International Journal of Wildland Fire* **17**(4), 500–514. doi:10.1071/WF08107

Hudak AT, Morgan P, Bobbitt MJ, Lentile L (2007*a*) Characterizing stand-replacing harvest and fire disturbance patches in a forested landscape: a case study from Cooney Ridge, Montana. In 'Understanding Forest Disturbance and Spatial Patterns: Remote Sensing and GIS Approaches'. (Eds MA Wulder, SE Franklin) Ch. 8, pp. 209–231. (Taylor & Francis: London)

Hudak AT, Morgan P, Bobbit MJ, Smith AMS, Lewis SA, Lentile LB, Robichaud PR, Clark JT, McKinley RA (2007*b*) The relationship of multispectral satellite imagery to immediate fire effects. *Fire Ecology* **3**(1), 64–90. doi:10.4996/FIREECOLOGY.0301064

Jenks GF (1967) The data model concept in statistical mapping. *International Yearbook of Cartography* **7**, 186–190.

Kasischke ES, Turetsky MR, Ottmar RD, French NHF, Hoy EE, Kane ES (2008) Evaluation of the composite burn index for assessing fire severity in Alaskan black spruce forests. *International Journal of Wildland Fire* **17**(4), 515–526. doi:10.1071/WF08002

Keane RE, Reinhardt E, Brown JK (1994) FOFEM – a first order fire effects model for predicting the immediate consequences of wildland fire in the United States. In 'Proceedings of the 12th Conference of Fire and Forest Meteorology', 26–28 October 1993, Jekyll Island, GA. pp. 628–631. (American Meteorological Society: Boston, MA)

Keane RE, Drury SA, Karau EC, Hessburg PF, Reynolds KM (2010) A method for mapping fire hazard and risk across multiple scales and its application in fire management. *Ecological Modelling* **221**, 2–18. doi:10.1016/J.ECOLMODEL.2008.10.022

Key CH, Benson NC (2006*a*) Landscape assessment: remote sensing of severity, the Normalized Burn Ratio. In 'FIREMON: Fire Effects Monitoring and Inventory System'. (Eds DC Lutes, RE Keane, JF Caratti, CH Key, NC Benson, LJ Gangi) USDA Forest Service, Rocky Mountain Research Station, General Technical Report RMRS-GTR-164. (Ogden, UT)

Key CH, Benson NC (2006*b*) Landscape assessment: remote sensing of severity, the Composite Burn Index. In 'FIREMON: Fire Effects Monitoring and Inventory System'. (Eds DC Lutes, RE Keane, JF Caratti, CH Key, NC Benson, LJ Gangi) USDA Forest Service, Rocky Mountain Research Station, General Technical Report RMRS-GTR-164. (Ogden, UT)

Kotliar NB, Simonson S, Chong G, Theobald D (2003) Effects on species of concern. In 'Hayman Fire Case Study'. (Ed. RT Graham) USDA Forest Service, Rocky Mountain Research Station, General Technical Report RMRS-GTR-114. (Ogden, UT)

Lachowski H, Hardwick P, Griffith R, Parsons A, Warbington R (1997) Faster, better, data for burned watersheds needing emergency rehab. *Journal of Forestry* **95**, 4–8.

Lentile LB, Holden ZA, Smith AM, Falkowski MJ, Hudak AT, Morgan P, Lewis SA, Gessler PE, Benson NC (2006) Remote sensing techniques to assess active fire characteristics and post-fire effects. *International Journal of Wildland Fire* **15**, 319–345. doi:10.1071/WF05097

Lentile LB, Morgan P, Hudak AT, Bobbit MJ, Lewis SA, Smith AMS, Robichaud PR (2007) Post-fire burn severity and vegetation response following eight large wildfires across the western United States. *Fire Ecology* **3**(1), 91–108. doi:10.4996/FIREECOLOGY.0301091

Lutes DC, Keane RE, Caratti JF, Key CH, Benson NC, Gangi LJ (Eds) (2006) FIREMON: Fire Effects Monitoring and Inventory System. USDA Forest Service, Rocky Mountain Research Station General Technical Report RMRS-GTR-164. (Fort Collins, CO)

Main WA, Paananen DM, Burgan RE (1990) Fire Family Plus. USDA Forest Service, North Central Forest Experiment Station, General Technical Report NC-138. (Saint Paul, MN)

McMaster R (1997) In Memoriam: George F. Jenks (1916–1996). *Cartography and Geographic Information Science* **24**(1), 56–59. doi:10.1559/152304097782438764

McNab WH, Avers PE (Comps) (1994) Ecological subregions of the United States: section descriptions. USDA Forest Service Administrative Publication WO-WSA-5. (Washington, DC)

Miller JD, Thode AE (2007) Quantifying burn severity in a heterogeneous landscape with at relative version of the Normalized Burn Ratio (dNBR). *Remote Sensing of Environment* **109**, 66–80. doi:10.1016/J.RSE.2006.12.006

Miller JD, Yool SR (2002) Mapping forest post-fire canopy consumption in several overstory types using multi-temporal Landsat TM and ETM data. *Remote Sensing of Environment* **82**, 481–496. doi:10.1016/S0034-4257(02)00071-8

Morgan PE, Hardy CC, Swetnam TW, Rollins MG, Long DG (2001) Mapping fire regimes across time and space: understanding coarse and fine-scale fire patterns. *International Journal of Wildland Fire* **10**, 329–342. doi:10.1071/WF01032

NWCG (National Wildfire Coordinating Group) (2003) Interagency Strategy for the Implementation of Federal Wildland Fire Management Policy. Available at http://www.nwcg.gov/branches/ppm/fpc/archives/fire_policy/index.htm [Verified 7 July 2010]

Ottmar RD, Burns MF, Hall JN, Hanson AD (1993) CONSUME users guide. USDA Forest Service, Pacific Northwest Research Station, General Technical Report GTR-PNW-304. (Portland, OR)

Pratt S, Holsinger L, Keane RE (2006) Using simulation modeling to assess historical reference conditions for vegetation and fire regimes for the LANDFIRE prototype project. In 'The LANDFIRE Prototype Project: Nationally Consistent and Locally Relevant Geospatial Data for Wildland Fire Management'. (Eds MG Rollins, CK Frame) USDA Forest Service, Rocky Mountain Research Station, General Technical Report RMRS-GTR-175. (Fort Collins, CO)

Reinhardt ED, Keane RE, Brown JK (1997) First Order Fire Effects Model: FOFEM 4.0 user's guide. USDA Forest Service, Intermountain Research Station, General Technical Report INT-GTR-344. (Ogden, UT)

Reinhardt ED, Keane RE, Brown JK (2001) Modeling fire effects. *International Journal of Wildland Fire* **10**, 373–380. doi:10.1071/WF01035

Roy DP, Boschetti L, Trigg SN (2006) Remote sensing of fire severity: assessing the performance of the Normalized Burn Ratio. *IEEE Geoscience and Remote Sensing Letters* **3**(1), 112–116. doi:10.1109/LGRS.2005.858485

Ryan KC, Noste NV (1985) Evaluating prescribed fires. In 'Proceedings, Symposium and Workshop on Wilderness Fire'. (Eds JE Lotan, BM Kilgore, WC Fischer, RM Mutch) USDA Forest Service, Intermountain Research Station, General Technical Report INT-182, pp. 230–238. (Ogden, UT)

Scott JH, Burgan RE (2005) Standard fire behavior fuel models: a comprehensive set for use with Rothermel's surface fire spread model. USDA Forest Service, Rocky Mountain Research Station, General Technical Report RMRS-GTR-153. (Fort Collins, CO)

Simard AJ (1991) Fire severity, changing scales, and how things hang together. *International Journal of Wildland Fire* **1**(1), 23–34. doi:10.1071/WF9910023

Sunar F, Ozkan C (2001) Forest fire analysis with remote sensing data. *International Journal of Wildland Fire* **22**(12), 2265–2277.

Turner MG, Hargrove WW, Gardner RH, Romme WH (1994) Effects of fire on landscape heterogeneity in Yellowstone National Park, Wyoming. *Journal of Vegetation Science* **5**, 731–742. doi:10.2307/3235886

Turner MG, Romme WH, Gardner RH (1999) Prefire heterogeneity, fire severity, and early post-fire plant reestablishment in subalpine forests of Yellowstone National Park, Wyoming. *International Journal of Wildland Fire* **9**(1), 21–36. doi:10.1071/WF99003

USFS (1995) Burned Area Rehabilitation Handbook. USDA Forest Service Handbook 2509.13, Amendment No. 2509.13–95–7. (Washington DC)

van Wagtendonk JW, Root RR, Key CH (2004) Comparison of AVIRIS and Landsat ETM+ detection ca pabilities for burn severity. *Remote Sensing of Environment* **92**, 397–408. doi:10.1016/J.RSE.2003.12.015

Zarriello TJ, Knick ST, Rotenberry JT (1995) Producing a burn/disturbance map for the Snake River Birds of Prey National Conservation Area. In 'Snake River Birds of Prey National Conservation Area Research and Monitoring Annual Report'. (USDOI Bureau of Land Management: Boise, ID)

Manuscript received 12 June 2009, accepted 24 January 2010